



堆浸水力学研究前沿：结构表征与模型仿真

缪秀秀^{1,3}, 吴爱祥¹, 杨保华²

(1. 北京科技大学 金属矿山高效开采与安全教育部重点实验室, 北京 100083;

2. 湖南涉外经济学院, 长沙 410205;

3. 中国科学院武汉岩土力学研究所, 岩土力学与工程国家重点实验室, 武汉 430071)

摘要: 随着堆浸提铜工艺的推广, 堆浸理论研究不断推进。渗流传质作为堆浸水力学过程的主线, 是影响矿物浸出速度的关键。当前, 矿堆水力学研究的前沿主要集中在矿堆散体结构表征及堆浸渗流传质过程的模拟。首先介绍以 CT 技术和计算机图像处理技术为核心的矿堆结构表征研究进展, 分析这一技术在矿堆结构表征上的局限; 其次阐述堆浸水力学过程仿真的发展, 分析传统模型存在的问题, 着重介绍孔隙尺度堆浸模型的种类和特征, 认为孔隙尺度模型是实现堆浸过程精细化、机制透明化的发展趋势。

关键词: 堆浸; 水力学; 结构表征; CT 技术; 渗流传质模型

文章编号: 1004-0609(2018)-11-2327-14

中图分类号: TF811; TD862

文献标志码: A

1 堆浸在铜金属回收上的应用

溶浸采矿技术可通过物理化学或生物等湿法处理手段, 有选择性地将有价金属矿物从低品位矿石、含矿废石甚至尾矿中溶解出来^[1]; 尤其适用于开发矿床禀赋差、规模小的多组分矿石; 而且相对传统选治手段, 该技术成本低、环境和大气污染小^[2-3]。堆浸是溶浸采矿最常见的工艺之一, 其工艺过程为在水不渗漏的场地上堆置适宜粒度的矿石或表外矿石; 通过从矿堆顶部向下喷洒溶浸液, 使溶浸液在矿堆的渗滤过程中溶解出矿石中的有用组份; 这些有用组分以离子的形式转入溶浸液中, 经过富集, 便可进一步通过萃取电积回收; 对于浸出金属浓度达不到萃取标准的贫液, 经离子浓度和 pH 调节后再循环喷淋。

铜矿为目前采用堆浸提取最成熟的矿种, 铜矿堆浸工艺在澳大利亚、智利、南非、秘鲁、美国等矿业发达国家得到广泛推广与应用^[4-5]。2010 年, 全球最大的 20 座铜矿中就有 9 座采用堆浸工艺处理其低品位矿石, 全球 450 万 t 铜通过溶浸采矿技术(主要为堆浸工艺)生产, 约占当年铜产量的 20%~30%^[6]。在我国, 采用堆浸提铜的成功应用例子却屈指可数。江西德兴

铜矿的浸出-萃取-电积(L-SX-EW)试验工厂^[7-8], 采用细菌堆浸未破碎的原生硫化铜矿表外矿或废石(平均品位 0.09%~0.25%), 堆场面积 75000 m², 堆高 80 m, 铜浸出率为 20.6%; 2010 年产阴极铜 1500 t, 生产成本小于 15000 元/t。紫金山铜矿于 2002 年初探溶浸提铜技术, 建成了电铜产量 1000 t/a 的生物冶金提铜试验厂, 2005 年正式建成了阴极铜产量 10000 t/a 的生物冶金提铜工厂, 2012 年该厂的阴极铜产量达 13000 t/a^[9-10]; 据 LIU 等^[11]报道, 2008 年上半年 1.4×10^6 t 品位为 0.5% 的铜矿石分 3 层(每层 8 m)入堆, 溶浸液 pH 0.85, 浸出周期 180 d 左右, 至 2010 年铜回收率已达 80%。由此可见, 铜矿堆浸仍有巨大发展潜力。

铜矿堆浸按处理矿石类型不同可分为废石堆浸和矿石堆浸两大类, 表 1 总结了这两类堆浸方式在工艺上的主要区别^[12-13]。通常溶浸液的喷淋强度为 4~20 L/(m²·h)^[14-16], 氧化铜矿的溶浸液一般为酸溶液(pH≈2), 硫化铜矿一般采用生物浸出, 浸矿微生物通过溶浸液接种入矿堆。大型矿堆至生命周期终止时, 占地可达几公顷, 堆高接近 100 m^[17]。

目的矿物的浸出率和浸出速度是反映堆浸工艺成功与否的主要指标^[18-19]。在矿堆这种大型结构中, 水力学对浸出剂的渗透起到至关重要的作用, 从而制约浸出剂与矿物反应浸出的过程; 而矿堆孔隙结构是决

基金项目: 中央高校基本科研业务费专项资金资助(FRF-BD-16-001A); 国家自然科学基金资助项目(51374035); 中国博士后基金资助项目(2018M632948)

收稿日期: 2017-07-24; 修订日期: 2017-11-15

通信作者: 吴爱祥, 教授, 博士; 电话: 010-62334680; E-mail: wuaixiang@126.com

表1 铜矿废石堆浸与矿石堆浸比较

Table 1 Comparison between dump leaching and heap leaching

Leach type	Target Cu mineral	Crushed	Heap height/m	Cu grade/%	Particle size/mm	Leaching time	Cu in pregnant leach solution/(g·L ⁻¹)	Cu recovery/%
ROM, oxides,								
Dump leach	secondary sulphide	No	8~75	0.1~0.4	30~1000	Several years	0.5~3	35~75
Oxides, secondary								
Heap leach	sulphide, agglomerated tailings	Yes	2~10	0.2~2.3	5~100	Several months to several years	1.5~8	40~90

定矿堆渗透率、持水特性、有效扩散系数等水力学参数的关键。堆浸矿石一般需要破碎至几个厘米大小,以揭露矿物颗粒^[20]。破碎不充分的矿石,颗粒内孔隙连通性差,溶浸液渗入阻力大,矿物浸出速度慢;破碎过度的粉矿,颗粒间孔隙率低,造成局部低渗,引起优势流。此外,未经破碎矿石或破碎不均匀的矿石堆中都存在孔隙(颗粒)大小差异大的问题,这类结构不均匀的矿堆,渗透性差异大,也易形成优势流^[21~23],导致矿物局部浸出。通常,矿石颗粒间的孔隙,其孔喉直径可达毫米至厘米级;颗粒内的孔隙,孔喉直径约为数微米;这两种尺度的孔隙构成了溶液渗流的主要通道,溶浸液在这两个尺度的孔隙中的流动规律是不同的^[24~25]。此外,反应动力学上,目标矿物类型、溶浸剂浓度、浸矿环境温度、矿石颗粒大小、矿物揭露程度、脉石矿物成分等是限制浸出效果的主要因素^[4, 26~27]。矿山的矿石类型决定了溶浸液的配方和最大可能浸出率;脉石中如含有可与溶浸剂反应的矿物,可导致溶浸剂扩散到目标矿物表面的浓度低于喷淋浓度。生物堆浸条件下,浸矿微生物的活性也是制约反应动力学的关键因素。矿堆内的溶氧、pH、堆内温度、浸矿微生物的营养成分和代谢产物浓度等都会影响微生物活性^[28~30]。

综上所述,矿堆结构及渗流传质水力学过程是堆浸工艺运作的基础,本文作者将从这两方面阐述堆浸研究进展,展望堆浸研究前沿。

2 矿堆结构表征

矿堆结构表征主要涉及无扰动成像技术、三维图像(二维图像序列)处理与三维图像计算三大内容。无

扰动成像技术是捕获矿堆二维图像序列,再现矿堆三维结构的基础;三维图像处理是结构表征的第二步,其目的是提取矿堆图像有效信息,是计算结构参数的前提。

当前较成熟的多孔介质无扰动成像技术包括计算机断层扫描(CT)技术、聚焦离子束-扫描电镜(FIB-SEM)、核磁成像(MRI)和粒子成像测速(PIV)等。其中CT技术在矿堆结构成像上应用最普遍,高精度工业微CT(μ CT)和粒子同步X射线CT(Synchrotron X-ray CT)的扫描精度可达微米级。FIB-SEM具有比CT更高的分辨率,可达纳米级,但显然其样本观察区域也很小^[31];在地球科学领域常用于化学成分和结构分析^[32~33],在矿堆结构表征方面较少见。相对CT和FIB-SEM,MRI和PIV技术并不属于矿堆结构成像技术的范畴,这两个技术常被用于分析多孔介质中的溶液流动过程。但MRI技术易受铁元素干扰,因而不适用于含铁量高的矿石(大部分金属矿石),而PIV技术无法穿透不透明介质。由此可见,MRI和PIV在堆浸分析的应用上具有很大局限。

CT矿堆三维图像处理所涉及的算法^[34~39]包括滤波算法、分割算法、中轴线算法等。由于成像设备扰动及样本抖动,CT图像通常存在一系列噪声,可通过各类滤波算法校正,例如高斯和中值滤波器可减弱CT图像最常见高斯/椒盐噪声。矿堆物相分割可通过阈值算法和分水岭算法实现。阈值算法主要用于区分孔隙、矿石、甚至矿石中的不同矿物,有直接基于灰度直方图的Otsu阈值、有基于图像灰度熵的最大熵阈值、还有基于邻域块的灰度分布的局部自适应阈值等^[34, 40~41]。若不同物相在灰度直方图上有明显的波峰/波谷,例如矿石和孔隙,大部分阈值算法均可实现较好的分割效果;若灰度直方图没有明显波峰/波谷,

如分割不同矿物时, 宜采用局部自适应阈值。阈值分割矿石和孔隙时, 接触的矿石在图像上表现为相互黏连的颗粒, 为实现颗粒分割(获得明确的颗粒边界), 可采用分水岭算法。分水岭算法操作的基础是原始图像的梯度图像, 由于矿石颗粒边缘粗糙, 基本分水岭算法常造成过度分割问题, 可采用基于标记的分水岭算法来改进^[36, 42]。中轴线算法主要是用于提取孔隙骨架, 为孔隙网络连通性和迂曲性分析提供基础, 此类算法相关的内容可参考 LINDQUIST 等^[43]提出的“焚烧”算法, BALDWIN 等^[44]提出的“细化”算法。

2.1 CT 技术在矿堆表征上的应用

CT 技术的应用由医学、材料领域, 逐渐推广到地球科学、环境科学以及岩土采矿等学科中。在岩土研究中, CT 技术被用于探索岩土中的孔(裂)隙结构^[45-50], 包括土壤中大孔隙的分布和统计, 岩石中裂隙的形态特征, 以及裂隙在热水力化耦合作用下的变化规律。目前已有研究可以实现渗流过程的可视化, 但均要求较快 CT 成像速度和极慢的渗流速度。借助粒子同步 X 射线 CT 技术, BARTELS 等^[51]实现了在砂岩和碳酸岩中以低浓度盐水驱油过程的成像, 实时显示了岩块孔隙饱和度的变化。由于粒子同步 X 射线 CT 成像非常快(可达常规 CT 时间的 1/10), 每帧 CT 图像间的差异较小, 通过时间解析重构算法, 并可再现流体在孔隙中的(短暂)动态过程。

当前, 基于 CT 技术的矿堆结构无损探测已成为溶浸体系研究的一大热点, 这方面研究主要借鉴了 CT 技术在岩土上的应用。虽然都是多孔介质, 但矿堆结构和岩石或土壤结构存在差异很大。一方面岩石的整体性较强, 是一种固体整体中分布着孔裂隙的结构, 而矿堆和土壤都是散体颗粒集合结构; 另一方面虽然土壤和矿堆都是散体结构, 但两者的颗粒级配差异非常大, 土壤中含有大量的黏土粒级的颗粒, 而矿堆中大部分是砾石粒级的颗粒, 且颗粒表面粗糙, 因而颗粒间的孔隙大小和形态差异也很大。最初 CT 技术普遍用于分析矿堆散体孔隙特征^[37, 52-57], LIN 等^[52]借助 CT 技术揭示了浸出过程中矿岩散体孔隙率的随浸柱高度的空间变化规律(见图 1)。MILLER 等^[54]通过 μCT 扫描微型浸柱, 分析了矿物揭露程度与矿石颗粒径的关系(见图 2)。杨保华^[57]使用医学 CT 扫描浸柱, 分析了二维孔隙率与浸柱断层分形关系, 同时也研究了矿石间孔隙的空间分布特征。

随 CT 扫描精度的不断提高, CT 技术逐渐被应用于揭露矿物颗粒内的物相和孔裂隙结构^[58-59]。KODALI 等^[60]借助 μCT 对不同破碎方式下氧化铜矿

和硫化铜矿颗粒内部的细观裂隙形成及其对最终浸出率的影响进行了研究。GHORBANI 等^[61]利用高精度 μCT 对颗粒内部裂隙空间分布特性以及矿物在颗粒内的分配进行了分析。GODEL 等^[62]利用高精度 X 射线 CT 和计算机三维图像分析技术, 分析了 Ni-Cu-PGE(铂族元素)单矿石颗粒内的矿物组分及分布规律(见图 3)。LIN 等^[63]使用 μCT 对单矿石颗粒在浸出过程中的几个阶段性进行扫描, 实现了矿石中矿物浸出过程的可视化(见图 4)。姚高辉^[56]利用 μCT 实验系统, 通过浸矿过程阶段性扫描, 对比了原矿石和制粒矿石在浸出过程中孔隙团的不同变化规律。

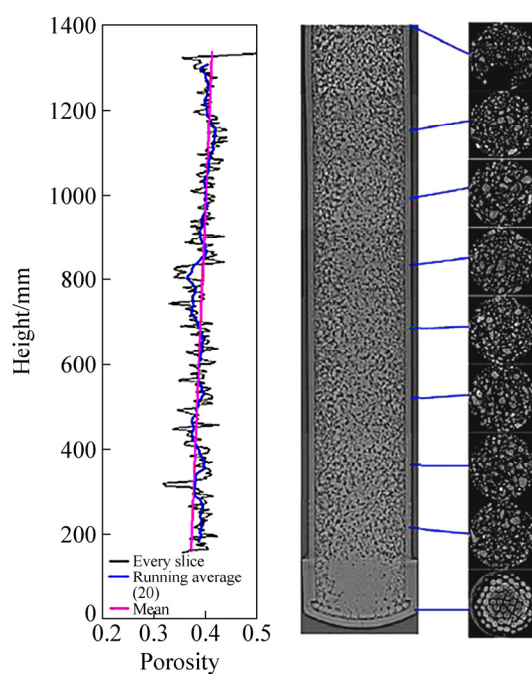


图 1 浸柱孔隙率空间变化分析^[52]

Fig. 1 Analysis of spatial variation of porosity within ore column^[52]

2.2 矿堆结构表征研究的局限

CT 在矿堆结构表征上的研究看似广泛, 但仍存在很多问题。一方面, 在 CT 图像处理和计算上, 一幅幅处理二维断层序列的伪三维的算法仍然非常普遍, 并未真正实现三维表征。例如, 分析孔隙和颗粒尺寸时, 孔隙和颗粒单体在二维断层上分割, 再计算尺寸分布。矿石颗粒间的孔隙和矿石颗粒的三维形状及其二维投影差异相对较小, 此时伪三维算法可能适用; 但是矿石颗粒内部往往孔裂隙并存, 裂隙结构在不同方向上的投影差异很大, 此时伪三维分析方法就可能失效。因此, 开发与推广高效三维结构表征方法对于处理复杂结构, 实现精细化表征非常有必要。

另一方面,不同尺度的矿堆结构表征尚无法统一。由于CT分辨率和扫描范围紧密相关,扫描分辨率越高,扫描样本范围越小。这一问题体现在矿堆结构上为:为观察矿石颗粒集间的结构,需采用较低扫描分

辨率,此时矿石颗粒内部结构不能被揭示;反之,观察矿石颗粒内结构时,尽管CT分辨率得到了充分的利用,但扫描范围小,无法体系颗粒集间的结构特征。因此,单纯依靠CT技术还不能同时观察不同尺度的

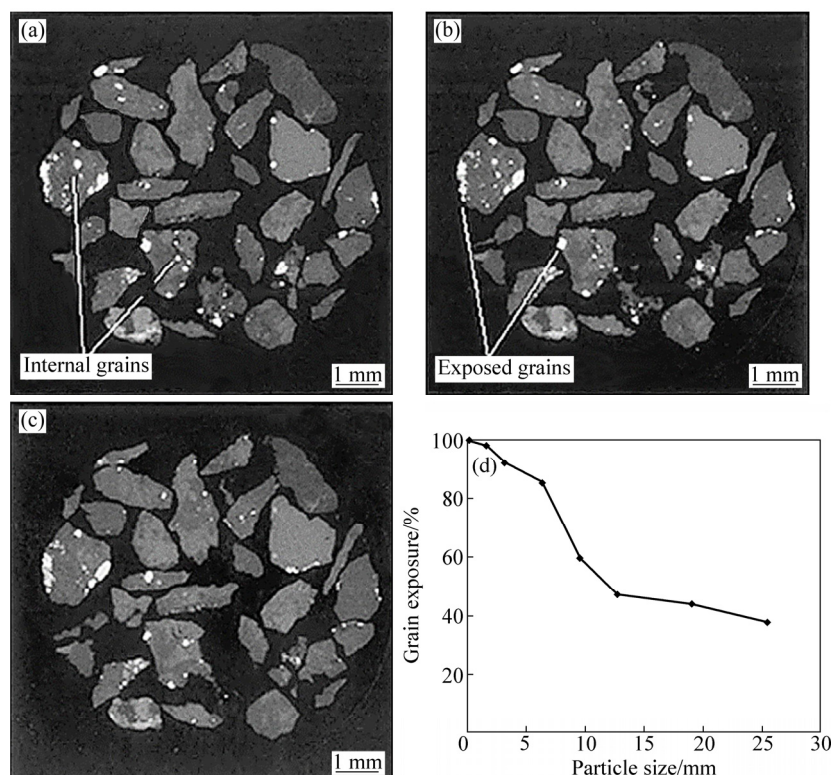


图2 矿物暴露程度分析^[54]

Fig. 2 Analysis of mineral exposure within ore column^[54]: (a)–(c) Slices from different heights ($z=0, 40, 80 \mu\text{m}$) of column; (d) Relation between mineral exposure and ore particle size

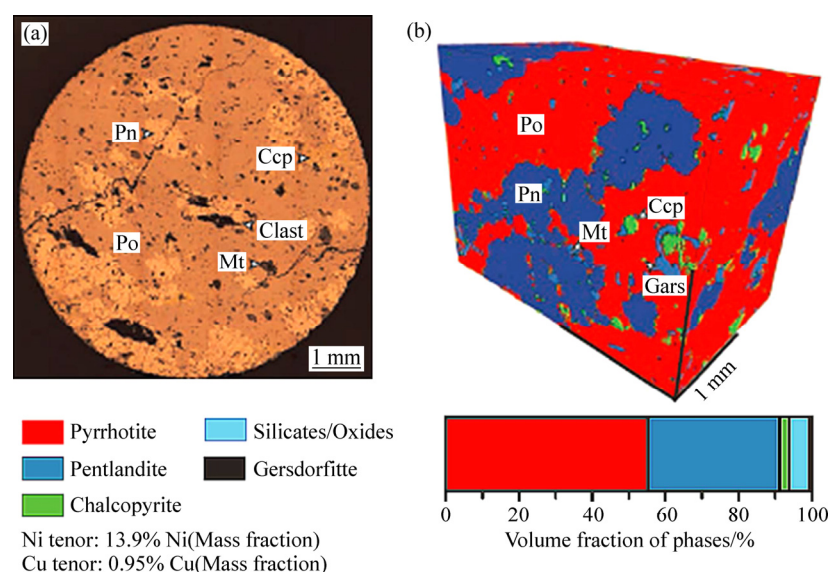
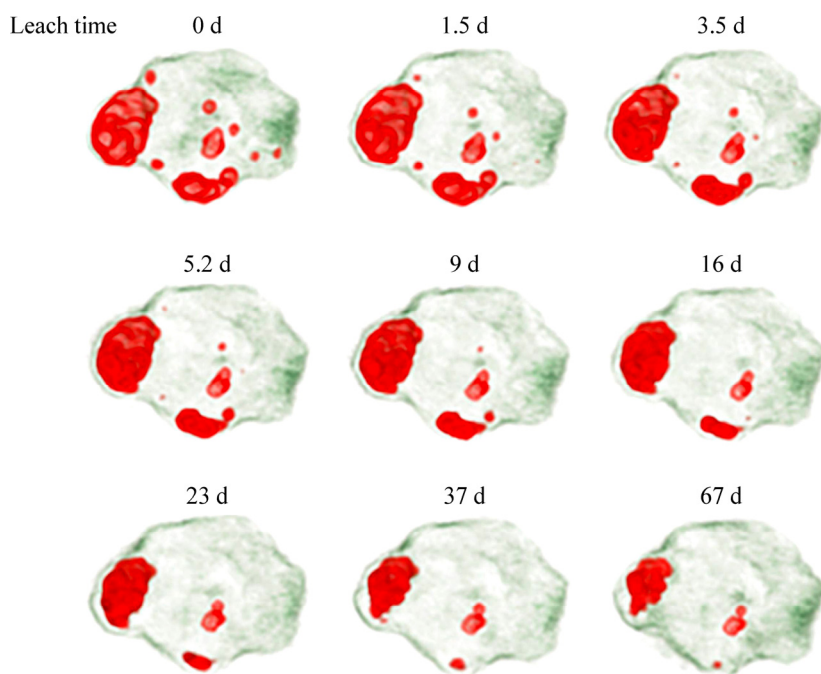


图3 分割Ni-Cu-PGE矿石内的矿物物相^[62]

Fig. 3 Minerals segmentation within Ni-Cu-PGE ore^[62]: (a) Raw CT slice; (b) Mineral phase segmentation from 3D region of interest

图4 实现单矿石阶段性浸出过程可视化^[63]Fig. 4 Visualised mineral dissolution from ore particle^[63]

矿堆结构,有必要从量化分析算法上入手实现不同尺度矿堆的关联,从多个尺度矿堆图像中提取关键特征,分析不同尺度结构参数间的相关性及独立性。

最后,虽然可以通过不同浸矿阶段的扫描分析矿堆结构变化规律,但CT扫描只能捕捉浸矿过程中某个瞬间(或短时)的矿堆结构,而浸矿是一个连续动态持久的过程,因此完全依靠CT技术实现浸矿过程的实时可视化仍不可行。基于无扰动成像及矿堆三维重构技术,建立浸矿过程多场耦合模型,开展浸出过程实时可视化分析,可能是技术经济可行的方案。

3 堆浸模型

大量研究从数学模型角度分析了堆浸的机制,按这些模型的研究尺度可分为矿堆模型、孔隙尺度模型、单矿物/单矿石模型^[64-65]。其发展可大致概括为:基于收缩核模型提出了单矿物/矿石的反应动力学模型;在单矿物/矿石反应动力学模型基础上,根据均匀多孔介质假设,提出矿堆/浸柱的物质与能量守恒模型;随CT技术的应用,基于非均质真实矿堆结构,提出了孔隙尺度堆浸模型,这类模型释放了均匀多孔介质矿堆的假设。在多年的研究累积中,这几类模型一直被更新完善。

3.1 单矿物/单矿石模型

单矿物/单矿石模型主要通过收缩核模型描述反应动力学^[66-69]。这类模型中,矿石或者矿物颗粒被视为理想球形颗粒,矿物均匀分布于颗粒内,主体溶浸液浓度恒定,矿物或矿石溶解可能由液膜内传质过程控制、多孔产物内扩散过程控制或未反应核表化学反应过程控制,如式(1)所示。这些早期收缩核模型是矿堆化学反应模型预测反应速度的基础。尽管实际浸出过程中,矿石颗粒的形态和物理特性均随反应在不断变化,但收缩核模型由于简单易用,仍然是最常用的估算浸出速度的方法^[70]。得益于CT技术,单矿物/单矿石模型在近期也有新的突破。LIN等^[71]利用CT图像重构了单颗矿石以及嵌布其中的矿物颗粒,并基于重构的矿石颗粒模拟了单矿石浸泡于静态恒定浓度溶浸液中的浸出过程(见图5),该模型松弛了收缩核模型关于理想球形颗粒和矿物均匀分布的限制,分别分析了化学反应控制和扩散控制的浸出过程的回收率。

$$\begin{cases} \frac{3k_l C_b}{\rho_s R} t = X_c \\ \frac{6D_e C_b}{\rho_s R^2} t = \left[1 - 3(1-X_c)^{\frac{2}{3}} + 2(1-X_c) \right] \\ \frac{k_s C_b}{\rho_s R} t = \left[1 - (1-X_c)^{\frac{1}{3}} \right] \end{cases} \quad (1)$$

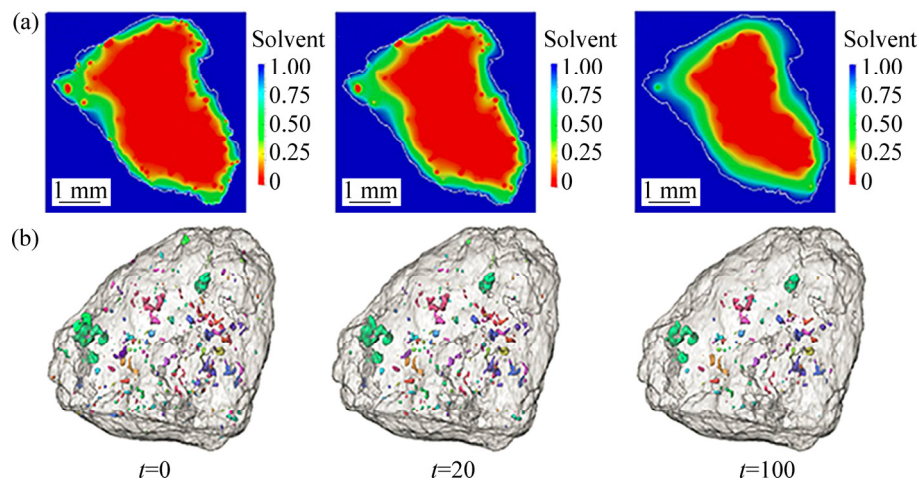


图5 基于重构单矿石的浸矿模型^[71]

Fig. 5 Particle leaching model based on reconstructed ore particle^[71]: (a) Solvent concentration predicted by simulation; (b) Mineral dissolution visualised by CT

式中: X_c 为矿物或矿石颗粒转化率; ρ_s 为矿物或矿石颗粒摩尔密度, mol/m³; R 为矿物或矿石颗粒初始半径, m; t 为时间, s; C_b 为外部恒定溶浸液浓度, mol/m³; k_t 为传质系数, m/s; D_e 为扩散系数, m²/s; k_s 为表面反应速度系数, m/s。

3.2 矿堆模型

矿堆尺度的模型一般假设整个矿堆为均质的多孔介质, 矿堆材料特性, 如矿堆密度、孔隙率、渗透率、热导率等, 都是各项同性的, 并且矿物均匀地分布于矿堆内。矿堆模型一般不考虑矿石在浸出过程中的形态和物理特性的变化, 采用矿石平均粒径代替整个矿堆的矿石级配, 利用简化的收缩核预测浸出反应速度^[26]。因此, 这类模型通常描述整个浸出体系的溶液、物质和热量流动平衡, 包括渗流、传质和传热 3 个基本控制方程, 如式(2)所示, 耦合模型涉及以溶液渗流和离子传递为主要研究内容的模型^[72-73], 以气体渗流和热量传递为主题的模型^[74-75], 还有渗流–传质–反应–传热全耦合的模型^[76-86]。LEAHY、BENNETT 和 CARIAGA 是研究堆浸全耦合模型较全面的三位学者, 他们建立了一系列基于均质假设经典的堆浸模型, 对优化堆浸工艺具有重要意义。CARIAGA 等^[77]针对铜矿堆浸工艺过程建立了气液两相渗流、硫酸和铜离子运移过程的模型, 可模拟不同条件下浸矿过程, 如矿堆高度、孔隙率、渗透率、饱和度、喷淋强度、浸矿剂浓度、反应速率等。BENNETT 等^[76]基于初期建立的环境土壤学和堆浸通用的气液两相渗流–反应传质模型, 开发了一个适用于铁离子氧化浸出辉铜矿和

黄铁矿的混合堆浸模型(见图 6), 并用柱浸实验校验了模型的有效性。该模型采用与浸柱内矿石粒径, 结合收缩核模型预测浸出反应速度, 同时可预测铁离子的沉淀和描述浸柱内的不饱和流行为。LEACHY 等^[80-84]专注于硫化铜矿的生物浸出模型。除了模拟矿堆内的渗流、反应和传质过程, 他们的模型还考虑了堆浸体系内温度、浸矿微生物和矿堆通气的相互作用。LEACHY 等^[85]于 2009 年建立了一个模拟黄铜矿堆浸过程中生成黄钾铁矾沉淀的模型, 该模型不仅可预测黄钾铁矾和其他铁离子的沉淀反应, 还描述了沉淀引起的宏观和细观孔隙堵塞, 孔隙堵塞改变渗流场和浸出速度的连锁过程。

$$\begin{cases} \frac{\partial \theta}{\partial t} + \nabla \cdot \mathbf{u} = 0 \\ \mathbf{u} = -K_s k_r \nabla (H_p + z) \\ \frac{\partial (\theta c_i)}{\partial t} + \nabla \cdot (-\mathbf{D}_{ei} \nabla c_i - \mathbf{D}_{di} \nabla c_i + \mathbf{u} \cdot \mathbf{c}_i) = R_i \\ \rho C_{sp} \frac{\partial T}{\partial t} + \nabla \cdot [-k_T \nabla T + (\rho_w C_{sp,w}) \mathbf{u} \cdot T] = Q \end{cases} \quad (2)$$

式中: θ 为矿堆含水率; t 为时间, s; \mathbf{u} 为堆内渗流速度矢量, m/s; K_s 为矿堆饱和渗透系数, m/s; k_r 为相对渗透系数; H_p 为孔隙水压力水头, m; z 为位置水头, m; c_i 为堆中离子 i 的浓度, mol/m³; \mathbf{D}_{ei} 为离子 i 在矿堆内的有效扩散系数, m²/s; \mathbf{D}_{di} 为离子 i 在矿堆内弥散系数, m²/s; R_i 为浸矿反应生成或消耗离子 i 的速度, mol/(m³·s); ρ 为矿堆密度, kg/m³; C_{sp} 为矿堆比热容, J/(K·kg); T 为堆内温度, K; k_T 为矿堆热导率, W/(m·K); ρ_w 为溶液密度, kg/m³; $C_{sp,w}$ 为溶液

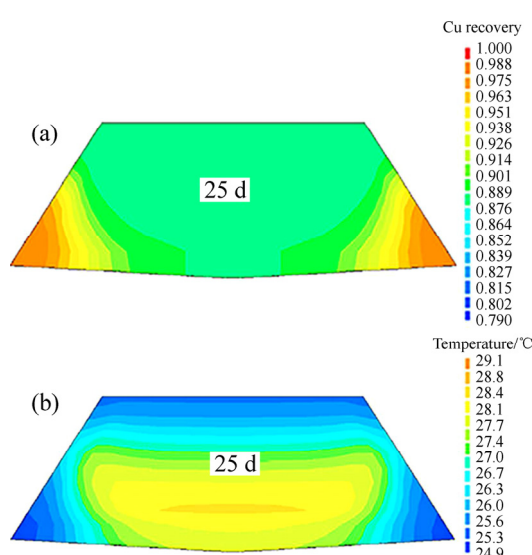
图 6 建立的堆浸多场耦合模型^[76]

Fig. 6 Multiphysical heap leaching model^[76]: (a) Copper leaching rate in 25 d; (b) Temperature distribution in 25 d

比热, $J/(K\cdot kg)$; Q 为浸矿反应释放或吸收热量的速度, W/m^3 。

3.3 孔隙尺度模型

孔隙尺度堆浸模型指的是矿堆几何体基于三维 CT 重构图像建立的模型。目前, 基于 CT 重构多孔介质的数值模型还只能实现单一的浸渗流、传质或传热过程的模拟, 而且主要在石油、化工、材料等领域中开展过一些研究。LARACHI 等^[87]通过 CT 技术重构了反应器孔隙结构, 并将孔隙结构抽象成孔隙体(节点)和孔喉(通道)的孔隙网络, 建立孔隙网络模型(Pore network model), 计算了固定床反应器中的非达西两层流流场, 如图 7(a)所示, 并称孔隙网络模型计算的流场与宏观测得的摩阻损失较相符。然而一些学者认为孔隙网络模型尽管求解速度快对计算能力要求低, 但对孔隙结构描述过于简单, 求解复杂孔隙流场可靠性差^[88-90]。MOSTAGHIMI 等^[91]通过有限差分(Finite

difference)法在三维 CT 孔隙上直接进行 Stokes 流模拟, 通过代数多重网格(Algebraic multigrid)算法求解流场, 如图 7(c)所示, 提出根据流场和孔隙结构预测砂堆散体、砂岩和碳酸岩渗透率的方法。

相对而言, 有限元(Finite element)大类模型求解流体更为成熟, 应用也更广。REAINI 等^[92]改良了有限体(Finite volume)法采用一种新的流体元(Volume-of-fluid)法在重构的矿堆几何体内模拟两相渗流。ACKERMANN 等^[93]基于 CT 重构的网眼陶瓷几何体模拟热量在固相中的传递, 并且根据模拟结果预测了该结构的热导率。ZARETSKIY 等^[94]采用有限元方法在 CT 重构的碳酸盐孔隙中模拟 Navier-Stokes 单相流和传质过程, 然而这个模型中液体流动和传质也不是完全耦合的。他们也采用代数多重网格算法和并行计算技术实现了求解过程的加速, 首先计算了孔隙内的流场, 再以流场解作为对流输入量, 模拟了对流扩散的传质过程。

目前, 直接孔隙模型在堆浸模拟中的应用案例很少, 且只实现了流场仿真, 孔隙内流动的基本控制为 Navier-Stokes 方程, 如式(3)所示。YANG 等^[95]采用有限元方法在重构的矿堆散体宏观孔隙内实现了渗流过程的可视化, 但也只是简单求解了速度场和压力在孔隙内的分布(见图 8)。LIN 等^[96]针对浸矿体系溶液非饱和渗流过程, 将 He-Chen-Zhang 改良 Lattice Boltzmann 模型应用于矿堆渗流求解, 在 CT 宏观孔隙基础上的建立了一个二维多相流模型, 可分析溶液在矿堆内的毛细现象。但是他们的模型都只利用了矿石颗粒间的孔隙, 忽视矿石内部的孔隙。

$$\begin{cases} \rho_w \frac{\partial \mathbf{v}}{\partial t} + (\rho_w \mathbf{v} \cdot \nabla) \mathbf{v} = \\ \nabla \cdot [-p \mathbf{I} + \eta_w (\nabla \mathbf{v} + (\nabla \mathbf{v})^T)] + \rho_w \mathbf{g} \\ \nabla \cdot \mathbf{v} = 0 \end{cases} \quad (3)$$

式中: ρ_w 为溶液密度, kg/m^3 ; η_w 为溶液黏度, $Pa\cdot s$; p 为孔隙水压, Pa ; \mathbf{v} 为溶液速度矢量, m/s ; \mathbf{g} 为重

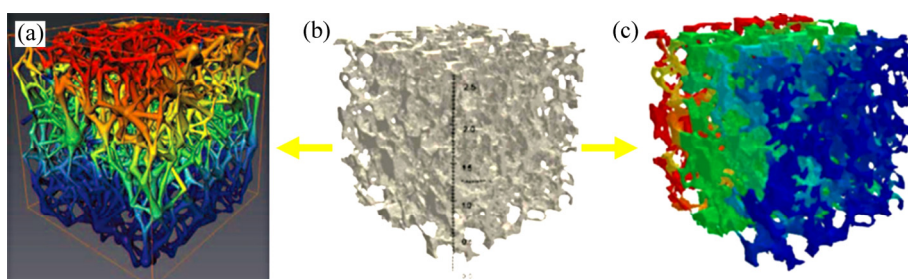


图 7 孔隙尺度模型

Fig. 7 Pore-scale models: (a) Pore-network model^[87]; (b) CT reconstructed pore structure; (c) Direct pore-scale model^[91]

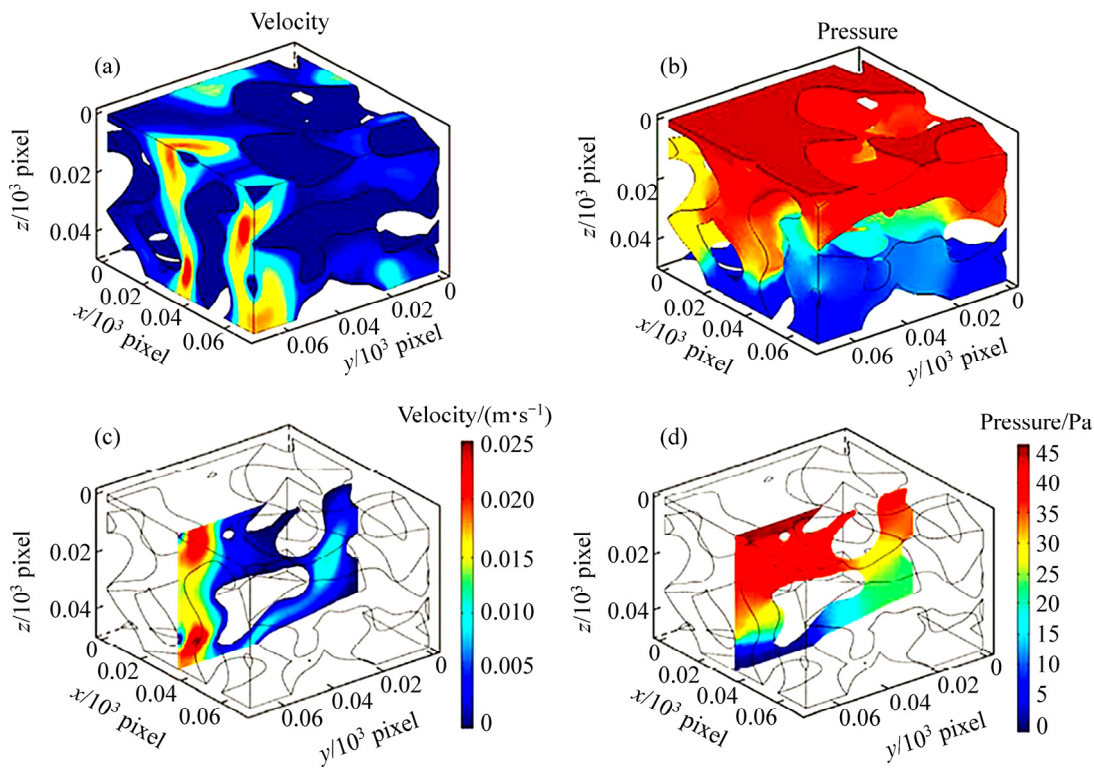


图8 有限元矿堆渗流模型^[95]

Fig. 8 Finite element pore-scale flow model^[95]: (a) Fluid velocity; (b) Pore-water pressure

力加速度矢量, m/s^2 ; t 为时间, s ; $\mathbf{I} = \begin{bmatrix} 1 & 0 & 0 \\ 0 & 1 & 0 \\ 0 & 0 & 1 \end{bmatrix}$ 。

MIAO 等^[25]认为构成矿堆结构中, 矿石颗粒间的宏观孔隙和颗粒内的细观孔隙均为关键渗流通道, 细观孔隙内的渗流过程不应被忽略。这一观点与 SHEIKHZADEH 等^[97]提出的双重介质矿堆假设相一致, 只是 SHEIKHZADEH 等的双重介质模型还是一种伪非均质结构, 该模型中细观和宏观孔隙结构都是均匀各向同性的。MIAO 等利用三维矿堆 CT 图像, 摆脱了结构的假设, 提出了矿堆的两级渗流模型。首先, 通过 CT 扫描获得矿石散体的宏观和细观孔隙, 分别模拟了宏观和细观孔隙中的 Navier-Stokes 流动, 并根据该流场解预测了宏观和细观结构在 3 个正交方向上的渗透率; 其次, 利用 Navier-Stokes 和 Brinkman's 的双区域控制方程求解宏细观孔隙并存矿堆中的两级渗流过程, 如式(4)所示。

$$\left\{ \begin{array}{l} \rho_w \frac{\partial \mathbf{v}_f}{\partial t} + (\rho_w \mathbf{v}_f \cdot \nabla) \mathbf{v}_f = \\ \nabla \cdot [-p_f \mathbf{I} + \eta_w (\nabla \mathbf{v}_f + (\nabla \mathbf{v}_f)^T)] + \rho_w \mathbf{g} \cdot \mathcal{Q}_f \\ \nabla \cdot \mathbf{v}_f = 0 \end{array} \right. \quad (4-1)$$

$$\left\{ \begin{array}{l} \frac{\rho_w}{\varepsilon_p} \frac{\partial \mathbf{v}_p}{\partial t} + \frac{\rho_w}{\varepsilon_p} \left((\mathbf{v}_p \cdot \nabla) \frac{\mathbf{v}_p}{\varepsilon_p} \right) = \\ \nabla \cdot \left[-p_p \mathbf{I} + \frac{\eta_w}{\varepsilon_p} (\nabla \mathbf{v}_p + (\nabla \mathbf{v}_p)^T) \right] - \frac{\eta_w}{\kappa_p} \mathbf{v}_p + \rho_w \mathbf{g} \cdot \mathcal{Q}_p \\ \nabla \cdot \mathbf{v}_p = 0 \end{array} \right. \quad (4-2)$$

式中: \mathcal{Q}_f 为宏观孔隙区域, 下标 f 表示宏观孔隙区域参数; \mathcal{Q}_p 为矿石(细观结构)区域, 下标 p 表示矿石区域参数; κ_p 为矿石渗透率, m^2 ; ε_p 为矿石孔隙率; ρ_w 为溶液密度, kg/m^3 ; η_w 为溶液黏度, $\text{Pa}\cdot\text{s}$; p 为孔隙水压, Pa ; \mathbf{v} 为溶液速度矢量, m/s ; \mathbf{g} 为重力加速度

$$\text{矢量, } \text{m/s}^2; t \text{ 为时间, } \text{s}; \mathbf{I} = \begin{bmatrix} 1 & 0 & 0 \\ 0 & 1 & 0 \\ 0 & 0 & 1 \end{bmatrix}.$$

综上所述, 由于重构的矿堆散体几何体形状极不规整, 无论是基于有限元、有限体或是 LB 的直接孔隙模型都存在一个共同的弊病, 那就是计算单元体数量多, 计算数据量大, 多场耦合模型往往是高度非线性, 求解速度慢。但是随着云计算资源和平行计算算法的普及, 相信计算能力上的限制将越来越弱化。此

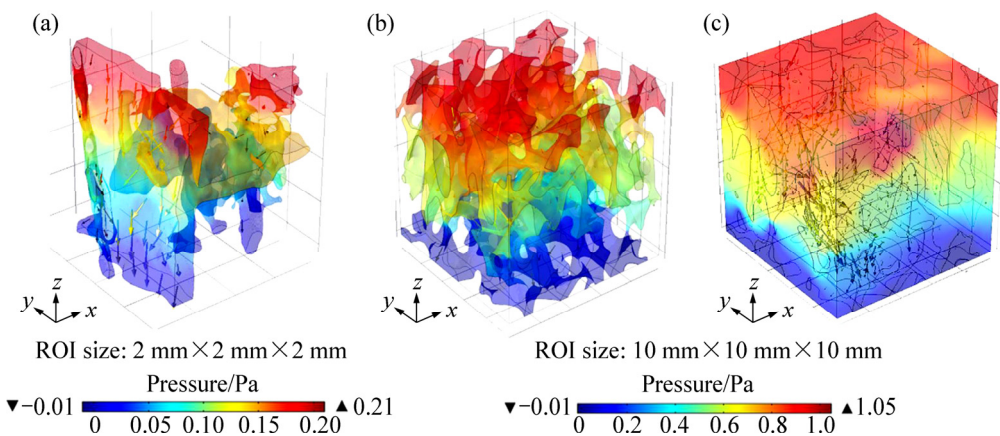


图9 矿堆两级渗流框架^[25]

Fig. 9 Two-stage flow constitute^[25]: (a) Micro-pore scale flow model; (b) Macro-pore scale flow model; (c) Dual-pore scale flow model

外, 传统均质模型的控制方程不再适用于孔隙尺度模型, 必须根据孔隙尺度模型的几何特征选择合适的控制方程。最后, 单一尺度的孔隙模型忽略了矿石内的孔隙, 这些细观孔隙对渗流对传质的作用如何, 仍有待深入研究。

4 结论及展望

铜矿堆浸工艺仍有很大的应用潜力, 堆浸理论研究也随着技术推广不断深入。CT技术、计算机图像处理方法和浸矿过程数值模拟是目前研究堆浸矿堆结构和浸矿水力学机制最前沿的几种手段。

CT作为一种高精度、无扰动的三维结构成像手段已被广泛应用于矿堆/矿石结构的探测, 结合计算机图像处理技术, 已成功实现矿石级配、矿堆孔隙率、矿物组分、矿堆分形特征等关键结构参数的分析。同时, 浸矿过程中矿石/矿堆的阶段性扫描也逐渐被用于分析矿堆结构动态变化规律。但是, 矿堆结构三维表征算法还有待推广与发展。而且矿堆细观结构和宏观结构的研究相互独立, 从算法角度上的跨尺度关联仍有待开展。此外, 浸矿是一个持久的动态过程, 不可能完全依靠CT分析浸出全过程, 发展基于重构矿堆的浸矿多场耦合模型较为可行。

传统堆浸模型尽管已经能模拟浸矿时化学、物理和生物交互的过程, 但是这类模型对矿堆结构和材料的假设过于理想, 把矿堆假设成连续均匀的多孔介质, 矿石颗粒视为完美球形, 认为矿堆密度、孔隙率、渗透率和热导率等材料参数各向同性。目前, 基于CT

重构矿堆发展的浸矿模型解放了矿堆结构的均质假设, 单颗粒尺度上, 已经模拟了矿石浸泡于恒定浓度溶液中的反应过程, 散体尺度上, 已实现溶液渗流过程的可视化。但是这类模型受计算能力限制发展较为缓慢, 多场耦合研究起步难。利用云计算资源, 结合高效的并行计算算法是解决计算能力限制的重要途径。此外, 如何处理并评价矿石内部细观孔隙重要性也是一个有待深入探讨的问题。

REFERENCES

- [1] 吴爱祥, 王洪江, 杨保华, 尹升华. 溶浸采矿技术的进展与展望[J]. 采矿技术, 2006, 6(3): 39–48.
WU Ai-xiang, WANG Hong-jiang, YANG Bao-hua, YIN Sheng-hua. Review and prospect of the development of solution mining[J]. Mining Technology, 2006, 6(3): 39–48.
- [2] BRIERLEY C. How will biomining be applied in future?[J]. Transactions of Nonferrous Metals Society of China, 2008, 18(6): 1302–1310.
- [3] MARSDEN J O. Energy efficiency and copper hydrometallurgy[C]//YOUNG C A, TAYLOR P R, ANDERSON C G, CHOI Y. proceedings of the 6th International Symposium on Hydrometallurgy. Arizona, USA: Society for Mining, Metallurgy, and Exploration, 2008: 29–42.
- [4] PRADHAN N, NATHSARMA K C, RAO K S, SUKLA L B, MISHRA B K. Heap bioleaching of chalcopyrite: A review[J]. Minerals Engineering, 2008, 21(5): 355–365.
- [5] WATLING H R. The bioleaching of sulphide minerals with emphasis on copper sulphides—A review[J]. Hydrometallurgy, 2006, 84(1/2): 81–108.
- [6] SCHLESINGER M E, KING M, SOLE K C, DAVENPORT W

- E. Extractive metallurgy of copper[M]. 5th ed. London, UK: Elsevier, 2011.
- [7] 孙业志, 吴爱祥, 黎剑华. 微生物在铜矿溶浸开采中的应用[J]. 金属矿山, 2001, (1): 3–5.
SUN Ye-zhi, WU Ai-xiang, LI Jian-hua. The application of microbe in the solution mining of copper ore[J]. Metal Mine, 2001(1): 3–5.
- [8] 徐茗臻. 湿法炼铜技术在江西铜业公司的应用[J]. 湿法冶金, 2000, 19(4): 26–30.
XU Ming-zhen. Application of copper hydrometallurgical process in JTCC[J]. Hydrometallurgy of China, 2000, 19(4): 26–30.
- [9] 刘大星. 我国铜湿法冶金技术的进展[J]. 有色金属(矿山部分), 2002, 54(3): 6–10.
LIU Da-xing. Development of hydrometallurgy in China[J]. Nonferrous Metals (Mining), 2002, 54(3): 6–10.
- [10] 阮仁满. 紫金山铜矿生物堆浸工业案例分析——相关动力学研究与多因素匹配[D]. 长沙: 中南大学, 2011.
RUAN Ren-man. A case study on bio-heapleaching practice of Zijinshan copper sulphide: Kinetics and process optimization[D]. Changsha: Central South University, 2011.
- [11] LIU X, CHEN B, WEN J, RENMAN R. Leptospirillum forms a minor portion of the population in Zijinshan commercial non-aeration copper bioleaching heap identified by 16S rRNA clone libraries and real-time PCR[J]. Hydrometallurgy, 2010, 104(3): 399–403.
- [12] DAVENPORT W G, KING M, SCHLESINGER M, BISWAS A K. Hydrometallurgical copper extraction: Introduction and leaching[M]//DAVENPORT W G, KING M, SCHLESINGER M, BISWAS A K. Extractive Metallurgy of Copper (4th edition). Oxford, UK: Pergamon, 2002: 289–305.
- [13] JOHN L. The art of heap leaching—The fundamentals[C]//Proceedings of the Conference on Percolation Leaching: The Status Globally and in Southern Africa. Muldersdrift, South Africa: The Southern African Institute of Mining and Metallurgy, 2011: 17–42.
- [14] HELLE S, KELM U, BARRIENTOS A, RIVAS P, REGHEZZA A. Improvement of mineralogical and chemical characterization to predict the acid leaching of geometallurgical units from Mina Sur, Chuquicamata, Chile[J]. Minerals Engineering, 2005, 18(13/14): 1334–1336.
- [15] KAPPES D W. Precious metal heap leach design and practice[C]//MULAR A L, HALBE D N, BARRATT D J. Proceedings of the Mineral Processing Plant Design, Practice, and Control. Vancouver, Canada: Society for Mining, Metallurgy, and Exploration, 2002: 1606–1630.
- [16] RAWLINGS D E. Characteristics and adaptability of iron- and sulfur-oxidizing microorganisms used for the recovery of metals from minerals and their concentrates[J]. Microbial Cell Factories, 2005, 4(1): 54–56.
- [17] BARTLETT R W. Metal extraction from ores by heap leaching[J]. Metallurgical and Materials Transactions B, 1997, 28(4): 529–545.
- [18] FREE M L. Hydrometallurgy: Fundamentals and applications[M]. New Jersey, USA: John Wiley & Sons, 2013.
- [19] PETERSEN J. Heap leaching as a key technology for recovery of values from low-grade ores—A brief overview[J]. Hydrometallurgy, 2015, 165: 206–212.
- [20] GHORBANI Y, MAINZA A N, PETERSEN J, BECKER M, FRANZIDIS J P, KALALA J T. Investigation of particles with high crack density produced by HPGR and its effect on the redistribution of the particle size fraction in heaps[J]. Minerals Engineering, 2013, s43/44(4): 44–51.
- [21] BOUMA J. Soil morphology and preferential flow along macropores[J]. Agricultural Water Management, 1981, 3(4): 235–250.
- [22] HERNÁNDEZ-LÓPEZ M F, ORTIZ C, BONILLA C A, GIRONÁS J, MUÑOZ J F. Modeling changes to the hydrodynamic characteristics of agglomerated copper tailings[J]. Hydrometallurgy, 2011, 109(109): 175–180.
- [23] WU A, YIN S, QIN W, LIU J, QIU G. The effect of preferential flow on extraction and surface morphology of copper sulphides during heap leaching[J]. Hydrometallurgy, 2009, 95(1/2): 76–81.
- [24] ILANKOON I M S K, NEETHLING S J. The effect of particle porosity on liquid holdup in heap leaching[J]. Minerals Engineering, 2013, 45(3): 73–80.
- [25] MIAO X, NARSILIO G A, WU A, YANG B. A 3D dual pore-system leaching model. Part 1: Study on fluid flow[J]. Hydrometallurgy, 2017, 167: 173–182.
- [26] GHORBANI Y, BECKER M, MAINZA A, FRANZIDIS J P, PETERSEN J. Large particle effects in chemical/biochemical heap leach processes—A review[J]. Minerals Engineering, 2011, 24(11): 1172–1184.
- [27] GHORBANI Y, FRANZIDIS J P, PETERSEN J. Heap leaching technology—Current state, innovations, and future directions: A review[J]. Mineral Processing & Extractive Metallurgy Review, 2015: 73–119.
- [28] GOVENDER E, BRYAN C G, HARRISON S T L. Quantification of growth and colonisation of low grade sulphidic ores by acidophilic chemoautotrophs using a novel experimental system[J]. Minerals Engineering, 2013, 48(7): 108–115.
- [29] GOVENDER E, BRYAN C G, HARRISON S T L. A novel experimental system for the study of microbial ecology and mineral leaching within a simulated agglomerate-scale heap bioleaching system[J]. Biochemical Engineering Journal, 2015, 95: 86–97.
- [30] SAND W, GEHRKE T. Extracellular polymeric substances mediate bioleaching/biocorrosion via interfacial processes involving iron(III) ions and acidophilic bacteria[J]. Research in Microbiology, 2006, 157(1): 49–56.

- [31] WIRTH R. Focused ion beam (FIB) combined with SEM and TEM: Advanced analytical tools for studies of chemical composition, microstructure and crystal structure in geomaterials on a nanometre scale[J]. *Chemical Geology*, 2009, 261(3): 217–229.
- [32] DUNN D, KUBIS A, HULL R. Quantitative three-dimensional analysis using focused ion beam microscopy[J]. *Introduction to Focused Ion Beams*, 2005: 281–300.
- [33] KOTULA P G, KEENAN M R, MICHAEL J R. Tomographic spectral imaging with multivariate statistical analysis: Comprehensive 3D microanalysis[J]. *Microscopy and Microanalysis*, 2006, 12(1): 36–48.
- [34] IASSONOV P, GEBRENEGUS T, TULLER M. Segmentation of X-ray computed tomography images of porous materials: A crucial step for characterization and quantitative analysis of pore structures[J]. *Water Resources Research*, 2009, 45(9): W09415.
- [35] ANDRÄ H, COMBARET N, DVORKIN J, GLATT E, HAN J, KABEL M, KEEHM Y, KRZIKALLA F, LEE M, MADONNA C. Digital rock physics benchmarks—Part I: Imaging and segmentation[J]. *Computers & Geosciences*, 2013, 50: 25–32.
- [36] KAESTNER A, LEHMANN E, STAMPANONI M. Imaging and image processing in porous media research[J]. *Advances in Water Resources*, 2008, 31(9): 1174–1187.
- [37] VIDELA A R, LIN C L, MILLER J D. 3D characterization of individual multiphase particles in packed particle beds by X-ray microtomography (XMT)[J]. *International Journal of Mineral Processing*, 2007, 84(1/4): 321–326.
- [38] YOUSSEF S, ROSENBERG E, GLAND N, BEKRI S, VIZIKA O. Quantitative 3D characterisation of the pore space of real rocks: Improved μ -CT resolution and pore extraction methodology[C]//The International Symposium of the Society of Core Analysts. Calgary, Canada, 2007: SCA2007–17.
- [39] KNACKSTEDT M, ARNS C, LIMAYE A, SAKELLARIOU A, SENDEN T, SHEPPARD A, SOK R, PINCZEWSKI W V, BUNN G. Digital core laboratory: Properties of reservoir core derived from 3D images[C]//Conference on Integrated Modelling for Asset Management. Kuala Lumpur, Malaysia: Society of Petroleum Engineers, 2004: SPE 87009.
- [40] SEZGIN M. Survey over image thresholding techniques and quantitative performance evaluation[J]. *Journal of Electronic Imaging*, 2004, 13(1): 146–168.
- [41] WANG W. Image analysis of aggregates[J]. *Computers & Geosciences*, 1999, 25(1): 71–81.
- [42] BEUCHER S, MEYER F. The morphological approach to segmentation: The watershed transformation[M]// *Mathematical Morphology in Image Processing*. New York: Marcel Dekker Inc., 1992: 433–481.
- [43] LINDQUIST W B, LEE S M, COKER D A, JONES K W, SPANNE P. Medial axis analysis of void structure in three-dimensional tomographic images of porous media[J]. *Journal of Geophysical Research Atmospheres*, 1996, 101(4): 8297–8310.
- [44] BALDWIN C A, SEDERMAN A J, MANTLE M D, ALEXANDER P, GLADDEN L F. Determination and characterization of the structure of a pore space from 3D volume images[J]. *Journal of Colloid and Interface Science*, 1996, 181(1): 79–92.
- [45] AL-RAOUSH R, ALSHIBLI K A. Distribution of local void ratio in porous media systems from 3D X-ray microtomography images[J]. *Physica A Statistical Mechanics & Its Applications*, 2006, 361(2): 441–456.
- [46] HIRONO T, TAKAHASHI M, NAKASHIMA S. In situ visualization of fluid flow image within deformed rock by X-ray CT[J]. *Engineering Geology*, 2003, 70(1/2): 37–46.
- [47] LIU J, POLAK A, ELSWORTH D, GRADER A. Dissolution-induced preferential flow in a limestone fracture[J]. *Journal of Contaminant Hydrology*, 2005, 78(1/2): 53–70.
- [48] PIERRET A, CAPOWIEZ Y, BELZUNCES L, MORAN C J. 3D reconstruction and quantification of macropores using X-ray computed tomography and image analysis[J]. *Geoderma*, 2002, 106(3/4): 247–271.
- [49] TIWARI P, DEO M, LIN C L, MILLER J D. Characterization of oil shale pore structure before and after pyrolysis by using X-ray micro CT[J]. *Fuel*, 2013, 107(9): 547–554.
- [50] CNUDDE V, BOONE M N. High-resolution X-ray computed tomography in geosciences: A review of the current technology and applications[J]. *Earth-Science Reviews*, 2013, 123(4): 1–17.
- [51] BARTELS W B, RÜCKER M, BERG S, MAHANI H, GEORGIADIS A, BRUSSEE N, COORN A, VAN DER LINDE H, FADILI A, HINZ C, JACOB A, WAGNER C, HENKEL S, ENZMANN F, BONNIN A, STAMPANONI M, OTT H, BLUNT M, HASSANIZADEH S M. Micro-CT study of the impact of low salinity waterflooding on the pore-scale fluid distribution during flow[C]//International Symposium of the Society of Core Analysts. Colorado, USA: SCA, 2016: 017.
- [52] LIN C L, MILLER J D, GARCIA C. Saturated flow characteristics in column leaching as described by LB simulation[J]. *Minerals Engineering*, 2005, 18(10): 1045–1051.
- [53] GARCIA D, LIN C L, MILLER J D. Quantitative analysis of grain boundary fracture in the breakage of single multiphase particles using X-ray microtomography procedures[J]. *Minerals Engineering*, 2009, 22(3): 236–243.
- [54] MILLER J D, LIN C L, GARCIA C, ARIAS H. Ultimate recovery in heap leaching operations as established from mineral exposure analysis by X-ray microtomography[J]. *International Journal of Mineral Processing*, 2003, 72(1/4): 331–340.
- [55] XU W, DHAWAN N, LIN C L, MILLER J D. Further study of grain boundary fracture in the breakage of single multiphase particles using X-ray microtomography procedures[J]. *Minerals Engineering*, 2013, s46/47: 89–94.

- [56] 姚高辉. 浸矿散体的微细结构演化规律与渗流特性研究[D]. 北京: 北京科技大学, 2012.
- YAO Gao-hui. Microstructure evolution of ore granular medium and its permeability during heap leaching[D]. Beijing: University of Science and Technology Beijing, 2012.
- [57] 杨保华. 堆浸体系中散体孔隙演化机理与渗流规律研究[D]. 长沙: 中南大学, 2010.
- YANG Bao-hua. The evolution mechanisms of the pore structure of granular ore media and seepage rules in heap leaching system[D]. Changsha: Central South University, 2010.
- [58] DHAWAN N, SAFARZADEH M S, MILLER J D, MOATS M S, RAJAMANI R K, LIN C L. Recent advances in the application of X-ray computed tomography in the analysis of heap leaching systems[J]. Minerals Engineering, 2012, 35(6): 75–86.
- [59] MILLER J D, GARCIA, LIN, C. L. Experimental evaluation of a mineral exposure model for crushed copper ores[M]//KAWATRA S K (editors). Advances in Comminution. Colorado, USA: Society for Mining, Metallurgy, and Exploration. 2006: 261–268.
- [60] KODALI P, DHAWAN N, DEPCI T, LIN C L, MILLER J D. Particle damage and exposure analysis in HPGR crushing of selected copper ores for column leaching[J]. Minerals Engineering, 2011, 24(13): 1478–1487.
- [61] GHORBANI Y, BECKER M, PETERSEN J, MORAR S H, MAINZA A, FRANZIDIS J P. Use of X-ray computed tomography to investigate crack distribution and mineral dissemination in sphalerite ore particles[J]. Minerals Engineering, 2011, 24(12): 1249–1257.
- [62] GODEL B. High-resolution X-ray computed tomography and its application to ore deposits: From data acquisition to quantitative three-dimensional measurements with case studies from Ni-Cu-PGE deposits[J]. Economic Geology, 2013, 108(108): 2005–2020.
- [63] LIN C, GARCIA C. Microscale characterization and analysis of particulate systems via cone beam X-ray microtomography (XMT)[C]//Proceedings of the Jan D, Miller Symposium—Innovations in Natural Resource Processing. Society for Mining, Metallurgy & Exploration, 2005: 421–432.
- [64] PETERSEN J, DIXON D G. Principles, mechanisms and dynamics of chalcocite heap bioleaching[M]//DONATI E R, SAND W. Microbial Processing of Metal Sulfides. Netherlands: Springer, 2007: 193–218.
- [65] PETERSEN J, DIXON D G. Modeling and Optimization of Heap Bioleach Processes[M]//RAWLINGS D E, JOHNSON D B. Berlin, Heidelberg: Springer, 2007: 153–176.
- [66] CASAS J M, VARGAS T, MARTINEZ J, MORENO L. Bioleaching model of a copper-sulfide ore bed in heap and dump configurations[J]. Metallurgical and Materials Transactions B, 1998, 29(4): 899–909.
- [67] DIXON D G, HENDRIX J L. A general model for leaching of one or more solid reactants from porous ore particles[J]. Metallurgical and Materials Transactions B, 1993, 24(1): 157–169.
- [68] MADSEN B W, WADSWORTH M E. A mixed kinetics dump leaching model for ores containing a variety of copper sulfide minerals[R]. Pittsburgh, USA: US Department of the Interior, Bureau of Mines, 1981.
- [69] PAUL B C, SOHN H, MCCARTER M K. Model for ferric sulfate leaching of copper ores containing a variety of sulfide minerals: Part I. Modeling uniform size ore fragments[J]. Metallurgical Transactions B, 1992, 23(5): 537–548.
- [70] MILLER G M. Ore geotechnical effects on copper heap leach kinetics[C]//YOUNG C, ALFANTAZI A, ANDERSON C, DREISINGER D, HARRIS B, JAMES A. proceedings of the 5th International Symposium on Hydrometallurgy. Vancouver, Canada: The Minerals, Metals & Materials Society, 2003: 329–342.
- [71] LIN Q, BARKER D J, DOBSON K J, LEE P D, NEETHLING S J. Modelling particle scale leach kinetics based on X-ray computed micro-tomography images[J]. Hydrometallurgy, 2016, 162: 25–36.
- [72] BOUFFARD S C, DIXON D G. Investigative study into the hydrodynamics of heap leaching processes[J]. Metallurgical and Materials Transactions B, 2001, 32(5): 763–776.
- [73] PANTELIS G, RITCHIE A I M, STEPANYANTS Y A. A conceptual model for the description of oxidation and transport processes in sulphidic waste rock dumps[J]. Applied Mathematical Modelling, 2002, 26(7): 751–770.
- [74] CATHLES L M, APPS J A. A model of the dump leaching process that incorporates oxygen balance, heat balance, and air convection[J]. Metallurgical and Materials Transactions B, 1975, 6(4): 617–624.
- [75] DIXON D G. Analysis of heat conservation during copper sulphide heap leaching[J]. Hydrometallurgy, 2000, 58(1): 27–41.
- [76] BENNETT C R, MCBRIDE D, CROSS M, GEBHARDT J E. A comprehensive model for copper sulphide heap leaching: Part 1 Basic formulation and validation through column test simulation[J]. Hydrometallurgy, 2012, s 127–128(18): 150–161.
- [77] CARIAGA E, CONCHA F, SEPÚLVEDA M. Flow through porous media with applications to heap leaching of copper ores[J]. Chemical Engineering Journal, 2005, 111(2/3): 151–165.
- [78] CARIAGA E, CONCHA F, SEPÚLVEDA M. Convergence of a MFE-FV method for two phase flow with applications to heap leaching of copper ores[J]. Computer Methods in Applied Mechanics & Engineering, 2007, 196(25): 2541–2554.
- [79] CROSS M, BENNETT C R, CROFT T N, MCBRIDE D, GEBHARDT J E. Computational modeling of reactive multi-phase flows in porous media: Applications to metals extraction and environmental recovery processes[J]. Minerals

- Engineering, 2006, 19(10): 1098–1108.
- [80] LEAHY M J, SCHWARZ M P, DAVIDSON M R. An air sparging CFD model for heap bioleaching of copper-sulphide[J]. Applied Mathematical Modelling, 2003, 30(11): 1428–1444.
- [81] LEAHY M J, DAVIDSON M R, SCHWARZ M P. A column bioleaching model for chalcocite—An investigation of oxygen limitation and bacterial inoculation on leaching[C]//Proceedings of the Bac-min 2004. Brisbane, Australia: Australasian Institute of Mining and Metallurgy, 2004: 175–178.
- [82] LEAHY M J, DAVIDSON M R, SCHWARZ M P. A model for heap bioleaching of chalcocite with heat balance: Bacterial temperature dependence[J]. Minerals Engineering, 2005, 18(13): 1239–1252.
- [83] LEAHY M J, SCHWARZ M P, DAVIDSON M R. An air sparging CFD model for heap bioleaching of chalcocite[J]. Applied Mathematical Modelling, 2006, 30(11): 1428–1444.
- [84] LEAHY M J, DAVIDSON M R, SCHWARZ M P. A model for heap bioleaching of chalcocite with heat balance: Mesophiles and moderate thermophiles[J]. Hydrometallurgy, 2007, 85(1): 24–41.
- [85] LEAHY M J, SCHWARZ M P. Modelling jarosite precipitation in isothermal chalcopyrite bioleaching columns[J]. Hydrometallurgy, 2009, 98(1): 181–191.
- [86] MIAO X, WU A, YANG B. Unsaturated flow and solute transport in a porous column using spherical ore particles[J]. International Journal of Minerals, Metallurgy, and Materials, 2014, 21(2): 113–121.
- [87] LARACHI F, HANNAOUI R, HORGUE P, AUGIER F, HAROUN Y, YOUSSEF S, ROSENBERG E, PRAT M, QUINTARD M. X-ray micro-tomography and pore network modeling of single-phase fixed-bed reactors[J]. Chemical Engineering Journal, 2014, 240(6): 290–306.
- [88] SHOLOKHOVA Y, KIM D, LINDQUIST W B. Network flow modeling via lattice-Boltzmann based channel conductance[J]. Advances in Water Resources, 2009, 32(2): 205–212.
- [89] RYAZANOV A V, DIJKE M I J V, SORBIE K S. Two-phase pore-network modelling: Existence of oil layers during water invasion[J]. Transport in Porous Media, 2009, 80(1): 79–99.
- [90] HELLAND J, RYAZANOV A, VAN DIJKE M. Characterization of pore shapes for pore network models[C]. 11th European Conference on the Mathematics of Oil Recovery. Bergen, Norway, 2008.
- [91] MOSTAGHIMI P, BLUNT M J, BIJELJIC B. Computations of absolute permeability on micro-CT images[J]. Mathematical Geosciences, 2013, 45(1): 103–125.
- [92] RAEINI A Q, BLUNT M J, BIJELJIC B. Direct simulations of two-phase flow on micro-CT images of porous media and upscaling of pore-scale forces[J]. Advances in Water Resources, 2014, 74: 116–126.
- [93] ACKERMANN S, SCHEFFE J, DUSS J, STEINFELD A. Morphological characterization and effective thermal conductivity of dual-scale reticulated porous structures[J]. Materials, 2014, 7(11): 7173–7195.
- [94] ZARETSKIY Y, GEIGER S, SORBIE K, FÖRSTER M. Efficient flow and transport simulations in reconstructed 3D pore geometries[J]. Advances in Water Resources, 2010, 33(12): 1508–1516.
- [95] YANG B, WU A, WANG C, NIU W, LIU J. Three-dimensional simulation of pore scale fluid flow in granular ore media with realistic geometry[J]. Transactions of Nonferrous Metals Society of China, 2012, 22(12): 3081–3086.
- [96] LIN C L, VIDELA A R, MILLER J D. Advanced three-dimensional multiphase flow simulation in porous media reconstructed from X-ray microtomography using the He-Chen-Zhang lattice boltzmann model[J]. Flow Measurement & Instrumentation, 2010, 21(3): 255–261.
- [97] SHEIKHZADEH G A, MEHRABIAN M A, MANSOURI S H, SARRAFI A. Computational modelling of unsaturated flow of liquid in heap leaching—Using the results of column tests to calibrate the model[J]. International Journal of Heat and Mass Transfer, 2005, 48(2): 279–292.

Recent advances in heap leaching research: Characterisation and modelling

MIAO Xiu-xiu^{1,3}, WU Ai-xiang¹, YANG Bao-hua²

(1. Key Laboratory of High-efficient Mining and Safety of Metal Mines, Ministry of Education,
University of Science and Technology Beijing, Beijing 100083, China;

2. Information Science and Engineering School, Hunan International Economics University, Changsha 410205, China;

3. State Key Laboratory for Geo-mechanics and Geo-technical Engineering, Institute of Rock and Soil Mechanics,
Chinese Academy of Sciences, Wuhan 430071, China)

Abstract: Theories on heap leaching has advanced over time with widely operated leach heaps, especially copper heaps. The flow and transport comprise the main research line running through the study on heap hydraulics, which is a critical influence on mineral dissolving rate. Currently, ore aggregate characterisation and coupled flow and transport modelling have become a frontier of the hydraulics research. The structure characterisation advances were reviewed by means of computed tomography (CT) and computational image processing, and the defects of both technologies that limit further progress on structure characterisation were analysed. Subsequently, the development of heap leaching models was traced. Limitation of conventional models was revealed, and the newly merged pore-scale modelling was introduced with emphasis on its features. It is believed that pore-scale model that takes advantage of CT geometry promises to be a potential direction for the advance of leaching models to visualise leaching process and illuminate the mechanisms.

Key words: heap leaching; hydraulics; structure characterisation; computed tomography; flow and transport model

Foundation item: Project(FRF-BD-16-001A) supported by the Fundamental Research Funds for the Central Universities;
Project(51374035) supported by the National Natural Science Foundation of China; Project
(2018M632948) supported by the Postdoctoral Science Foundation of China

Received date: 2017-07-24; **Accepted date:** 2017-11-15

Corresponding author: WU Ai-xiang; Tel: +86-10-62334680; E-mail: wuaixiang@126.com

(编辑 王 超)